Hydrology Research

Hydrology Research Vol 53 No 11, 1357 doi: 10.2166/nh.2022.038

Influence of reservoir impoundment on rainfall erosivity in the Three Gorges Reservoir region of China

Guangyi Jiang[a,b,c], Jiaorong Lv[a,d,*,†], Xiubin He[a] and Yuhai Bao[a]

[a] Key Laboratory of Mountain Surface Processes and Ecological Regulation, Institute of Mountain Hazards and Environment, Chinese Academy of Sciences, Chengdu, Sichuan, China
[b] Chongqing Eco-environment Monitoring Station of Soil and Water Conservation, Chongqing 401147, China
[c] University of Chinese Academy of Sciences, Chengdu, Sichuan, China
[d] Present/permanent address: No. 9, 4th Section, South Renmin Road, Wuhou District, Chengdu, Sichuan, China
*Corresponding author. E-mail: lvjiaorong@imde.ac.cn
[†] Jiaorong Lv contributed equally to this work and should be considered as co-first authors.

ABSTRACT

New dammed reservoirs are expected to have a significant effect on the regional hydrocycle, but the detailed patterns may not be well understood. Regional climate change is likely to cause soil erosion uncertainty by affecting rainfall erosivity. In the present study, local precipitation and rainfall erosivity were investigated to determine the impounding influence of the Three Gorges Reservoir. Daily erosive precipitation, from 1980 to 2020, was categorized into four intensity levels (light, moderate, heavy, and very heavy), as well as extreme rainfall, to understand their contribution to erosivity. It was found that the impoundment significantly affected local precipitation, with both heavy precipitation and the relative erosivity showing a substantial declining trend (Sen's slope = 2.141, $p < 0.05$). The Mann–Kendall test indicated an abrupt change point around the year 2002, evidencing the effect of the reservoir impoundment (since 2003). Reservoir impoundment redistributed the intensity levels of erosive precipitation, leading to a 24.3% decrease in the erosivity of heavy precipitation and an 8.2% increase in the moderate category. The unimodal distribution of monthly precipitation was altered to a bimodal distribution with peaks in July and September, resulting in a longer but lower-risky erosion period of high concern. The fluctuations of Rx1day and Rx5day were obviously flattened after impoundment, with a 54.2% peak reduction in relative erosivity on average. Results indicated that heavy rainfall (including extreme rainfall) was reduced, and annual precipitation and erosivity both had a more even seasonal distribution following reservoir impoundment.

Key words: extreme precipitation, impoundment, rainfall erosivity, temporal variation, Three Gorges Reservoir

HIGHLIGHTS

- The Three Gorges Reservoir impoundment significantly affected local precipitation.
- The abrupt change point (Mann–Kendall test) was around the year 2002.
- The heavy precipitation and the relative erosivity both substantially declined.
- The monthly precipitation distribution was altered from unimodal to bimodal.
- The interannual fluctuations of extreme rainfall were significantly reduced.

GRAPHICAL ABSTRACT

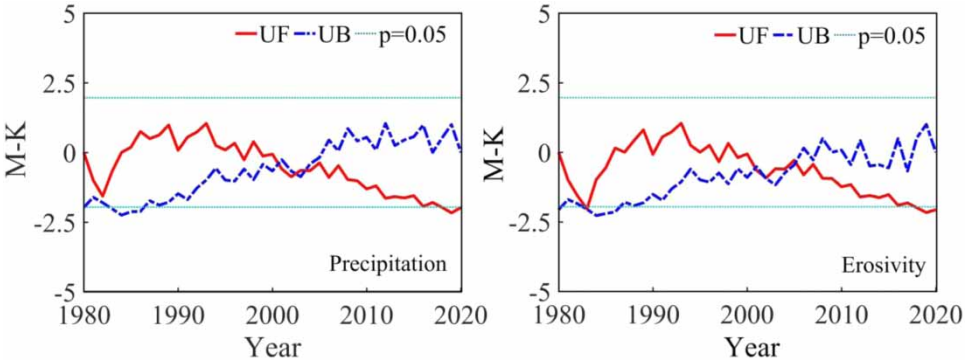

INTRODUCTION

Spatiotemporal variations in global and regional precipitation are among the most relevant aspects of climate change in warming conditions (Pendergrass *et al.* 2017; Yao *et al.* 2020). An upward trend of rainfall extremes is frequently responsible for natural hazards such as floods, landslides, and debris flows (Donat *et al.* 2017; Pendergrass *et al.* 2017). Apart from global warming, other anthropogenic factors such as dam construction are also important causes of extreme precipitation variation (Hossain *et al.* 2010). The moisture-heat exchange above the water surface area becomes more intense after reservoir impoundment, and therefore, evaporation changes coupled with significant land use and complicated surrounding topography may alter the regional precipitation pattern (Gangoiti *et al.* 2011; Keller *et al.* 2021). Hossain *et al.* (2010) and Yigzaw *et al.* (2012) demonstrated that extreme precipitation (99th percentile) showed a 4% increase per year after dam construction. Pizarro *et al.* (2013) compared the intensity of extreme precipitation located near water bodies to those away from water bodies, finding higher precipitation intensity at locations closer to water bodies.

The Three Gorges Reservoir (TGR) area – which contains Three Gorges Dam (TGD), the largest hydroelectric project in the world (Xu *et al.* 2013) – has a water surface area of 1,084 km^2 (Miller *et al.* 2005). Specific field experiments and idealized numerical simulations suggested that the climatic influence of the TGR would be primarily within tens of kilometers of the Yangtze River waterway (Miller *et al.* 2005; Wu *et al.* 2006). There are studies that reported variations in precipitation and extreme precipitation over the TGR area (Fang *et al.* 2010; Zhao & Shepherd 2012). Some of these indicated no significant change in precipitation and precipitation pattern after the TGD began operating (in the year 2003) (Miller *et al.* 2005; Song *et al.* 2020). However, a numerical simulation by Wu *et al.* (2006) demonstrated that the TGD construction reduced precipitation in the vicinity of the TGR after the water impounding (135 m) in June 2003. Extreme precipitation in the TGR area was found by Lv *et al.* (2018) to have become more frequent since 1985 due to climate warming.

The TGR has been impounding water since 2003 (Xu *et al.* 2013). The extensive water surface areas of reservoirs can influence regional convective patterns and associated thunderstorms by widening open water bodies and enhancing the moisture supply for precipitation, hence serving as a feeder for precipitation (Miller *et al.* 2005; Woldemichael *et al.* 2014). Moreover, above the water surfaces, the available convective potential energy is increased, which in turn might induce more precipitation (Degu *et al.* 2011; Hsu *et al.* 2016). However, most of the aforementioned studies of the effects of dam operation on local precipitation only considered precipitation datasets before 2010 in the TGR area (Xiao *et al.* 2010; Liu *et al.* 2020). This is far from sufficient to understand the local precipitation and extreme precipitation changes before and after the impoundment of the reservoir. A few studies used data from more recent time series, but did not reveal the rainfall change before and after impoundment due to the different research aim (e.g., Lv *et al.* 2018) or the temporal constraints of data series (Song *et al.* 2020). Therefore, references discussing the effects of reservoir impoundment on the local climate in the TGR area are still very limited.

The TGR area has one of the most serious soil erosion problems in China (Shi *et al.* 2021). The annual amount of eroded soil is as high as 150 million tons in this area (Xiao *et al.* 2020). Rainfall erosivity, considering rainfall amounts and intensities, is an important parameter in soil erosion risk assessments for future land uses and climate change (Shin *et al.* 2019; Xu *et al.* 2021). In the TGR area, the changes in the amounts, intensities, and frequencies of precipitation are influenced by TGD operation and certainly will be bound to affect the rainfall erosivity and degree of soil erosion. However, the previous studies have

paid more attention to the long-term change trends of annual precipitation (Fang *et al.* 2010; Degu *et al.* 2011; Zhao & Shepherd 2012), while very few studies focused on the erosive precipitation variation influenced by the dam operation, including the composition of the erosive rainfall and its respective erosivity contribution (Liu *et al.* 2020).

Some studies have shown that extreme rainfall plays a key role in soil erosion, and most soil erosion usually results from a few extreme rainfall events (Shi *et al.* 2021; Xu *et al.* 2021). The effects of extreme rainfall on soil erosion have become one of the main concerns addressed in soil erosion studies (Gu *et al.* 2016). Studies referring to extreme rainfall in the TGR area are relatively few (Fang *et al.* 2010; Lv *et al.* 2018), indicating an increase both in frequency and intensity of the extreme precipitation. The impact of the TGR impoundment on extreme precipitation has not been clarified. Therefore, the variations of heavy precipitation, including extreme precipitation, wait to be revealed, along with the corresponding erosivity contribution pre- and post-impoundment. It will be of great practical significance to understand reservoir effects on local soil erosion, to further reduce the uncertainty of soil erosion in the future.

Consequently, in the present study, the interannual and seasonal variability of erosive precipitation, classified into different intensity categories (light, moderate, heavy, and very heavy), are analyzed based on the latest daily precipitation data series (as of 2020). Furthermore, the erosivity contribution of different categories of rainfall including extreme precipitation is examined by using a calculation model of rainfall erosivity that is based on daily rainfall. Besides, the changes in precipitation and erosivity before and after the reservoir impoundment, as well as how they influenced by impoundment are discussed. The results from the present study can help understand the influence of TGR impoundment on local precipitation characteristics, especially erosive rainfall events. This will be a guide towards more appropriate strategies to address soil and water loss to provide a scientific basis for ecological security and regional sustainable development in the TGR region.

STUDY AREA

The TGR (28°31′–31°44′N, 105°50′–111°40′E) is a typical river reservoir (Figure 1). The reservoir area includes the middle and upper reaches of the Yangtze River from Chongqing Jiangjin in the west to Yichang, Hubei in the east, with a length of 660 km and an average width of 1.1 km across the Yangtze River. The study area, Wanzhou district of Chongqing (30°24′–31°14′N, 107°55′–108°53′E, 3,457 km^2), is located in the center of the TGR region and falls in the mountainous areas (Figure 1). The climate of the study area is humid mid-subtropical with alternating winter and summer monsoons and obvious seasonal changes in temperature and precipitation. The average annual temperature is 17.7 °C and the precipitation is 1,200–1,400 mm. The erodible purple soil is the dominant soil type in the Wanzhou district, with an annual soil loss of 5.722 million tons, making this one of the most serious soil erosion areas in the TGR.

The reservoir has been in partial operation since June 2003, and the water level rose from 66 to 135 m (Figure 2). From 2009, the TGR has inundated 632 km^2 of land with a normal water level of 175 m and a water storage capacity of 39.3 billion m^3. The extensive water surface may have a certain impact on the climate of the reservoir and its surrounding area, but the extent of the impact the reservoir can have on the local climate remains controversial. In the present study, the period of 1980–2002 is the time series before impoundment, and the period of 2003–2020 is the time series after impoundment. Based on this, the response of local rainfall characteristics (in the Wanzhou District) to the impoundment of the TGR is studied.

DATA AND METHODS

Data

In the present study, we used daily precipitation data from the Wanzhou station in Chongqing City, China for the period of 1980–2020 (Figure 2). The data were obtained from the China Meteorological Data Sharing Service System (http://www.cma.gov.cn/2011qxfw/2011qsjgx/) and subjected to quality control and homogeneity tests using RClimDex and RHtest software, respectively. These two pieces of software are freely available from the Expert Team on Climate Change Detection and Indices (ETCCDI) website (https://www.wcrp-climate.org/etccdi).

Precipitation indices and trend calculation

Percentile-based thresholds have commonly been used to define extreme events in past studies. For example, heavy precipitation events were often defined as the top 5% of events, and very heavy precipitation events as the top 1% (Martin *et al.* 2016; Wu *et al.* 2016). In the present study, we used three percentile values (85, 95, and 99%) were used as thresholds to divide all erosive precipitation events (daily precipitation $\geq$10 mm) into four non-overlapping categories: light, moderate, heavy, and

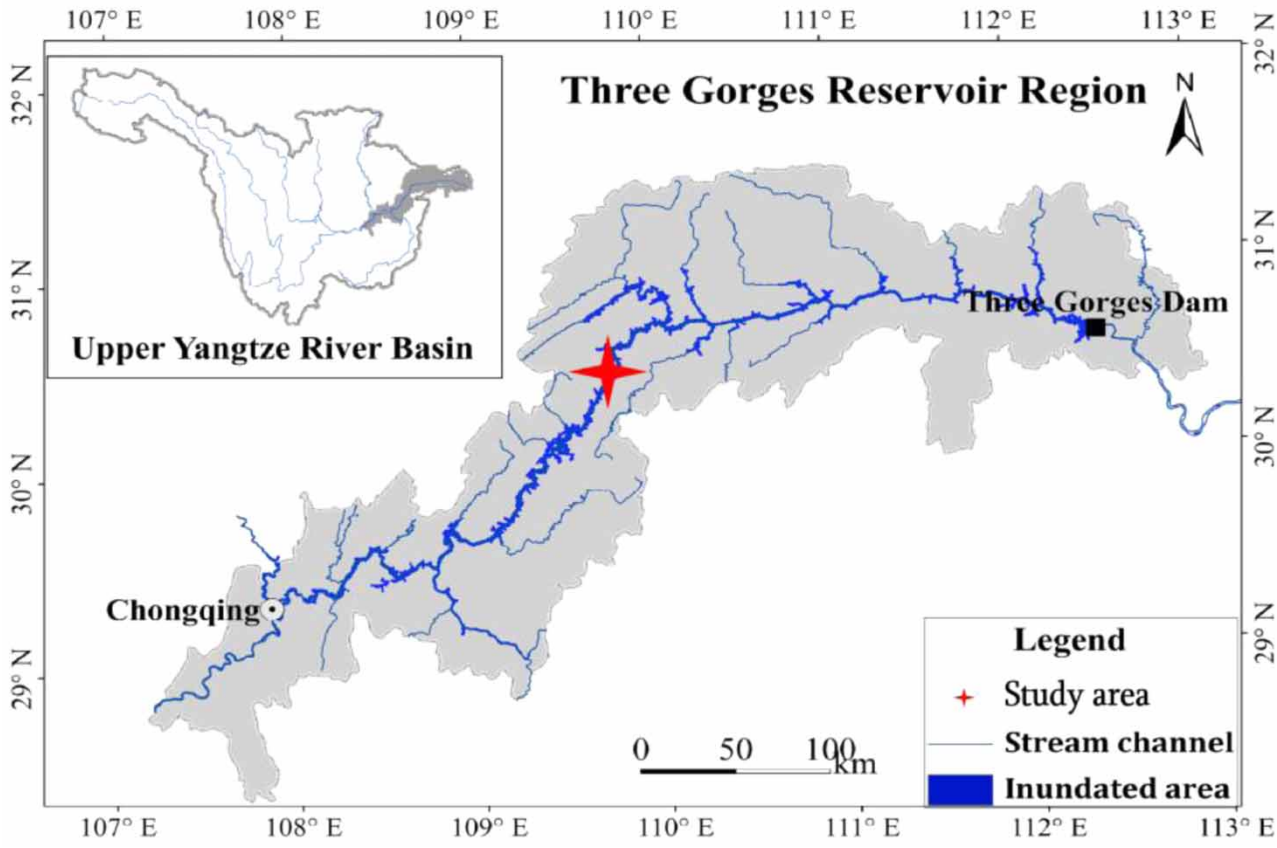

Figure 1 | Location of the Three Gorges Reservoir area and the location of Wanzhou district.

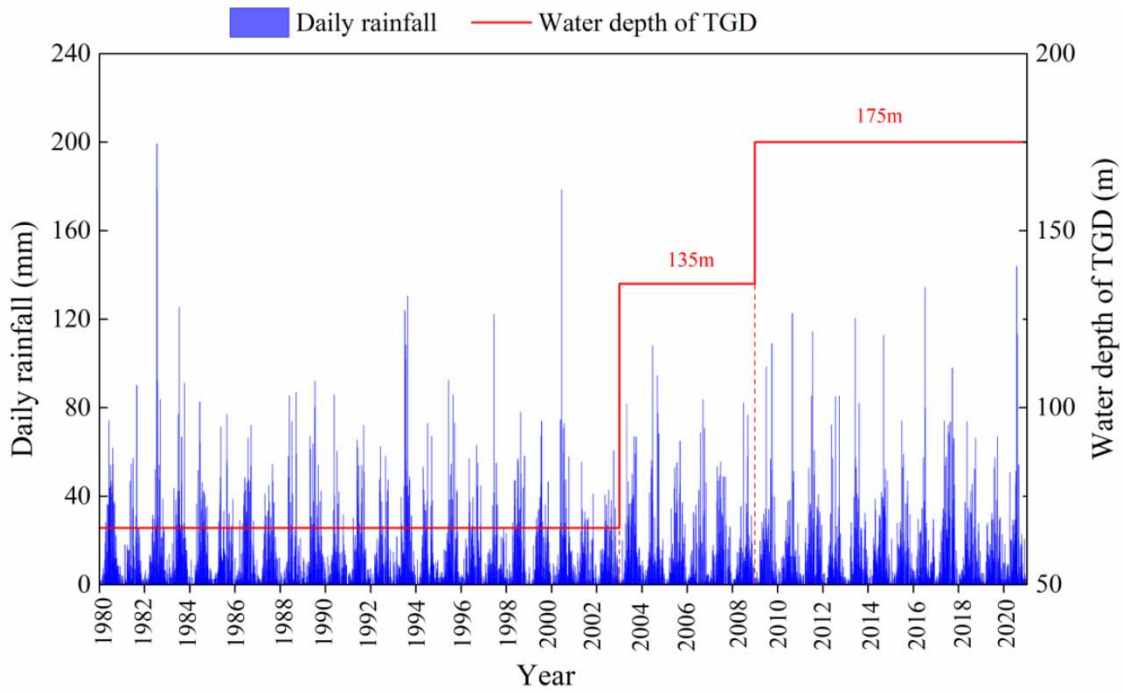

Figure 2 | The storage process line of Three Gorges Reservoir as well as the daily rainfall process line for the period of 1980–2020.

very heavy. Days with precipitation totals ≥0.1 mm were treated as precipitation events. The variables examined in this study were defined as follows:

- Light precipitation: the precipitation amount per year below a threshold value of the 85th percentile of daily precipitation amounts distribution from 1980 to 2020 (mm, <85th percentile).
- Moderate precipitation: the total amount of precipitation from the moderate precipitation days (mm, 85th–95th percentile).
- Heavy precipitation: the total amount of precipitation from heavy precipitation days (mm, 95th–99th percentile).
- Very heavy precipitation: the total amount of precipitation from very heavy precipitation days (mm, ≥99th percentile).

In order to study the rainfall erosivity contribution of a single/short-term heavy rainfall, two extreme precipitation indices Rx1day and Rx5day were used, defined as annual maximum 1-day and maximum consecutive 5-day precipitation, respectively, and are two of the recommended indices by the ETCCDMI to investigate extreme climatic variations.

One common non-parametric method for trend detection adopted for this study is the Mann–Kendall (M-K) test (Mann 1945; Kendall 1975). The M-K test can be used to detect the existence of statistically significant trends (Liu *et al.* 2020). However, it does not provide magnitudes of the trend slope. Therefore, another commonly used non-parametric approach, namely the Theil–Sen estimator (Sen 1968; Theil 1992), was used to estimate the slope of the trends.

Rainfall erosivity model

The rainfall erosivity was calculated using a Xie *et al.* (2016) model. The accuracy of the R factor was proven to be much higher when the seasonality was taken into consideration. This model, which has been effectively and widely applied in China (Xu *et al.* 2021; Zhang *et al.* 2021), was employed to calculate half-month rainfall erosivity based on daily rainfall. The equations of the model are as follows:

$$R_{\text{day}} = \alpha P_{\text{d}}^{1.7265} \tag{1}$$

$$R = \sum R_{\text{day}} \tag{2}$$

where R_{day} and R are daily and yearly rainfall erosivities, respectively (MJ mm ha^{-1} h^{-1} y^{-1}); α is a parameter that equals 0.3937 in the warm season (May–September) and 0.3101 in the cool season (October–April), which are the averages based on the rainfall data for 16 stations in China (Xie *et al.* 2016); P_{d} is the daily precipitation ≥10 mm (Xie *et al.* 2016), which is considered as erosive rainfall (mm) (Yin *et al.* 2019).

RESULTS

Interannual variability in precipitation and erosivity

During the period of 1980–2020, the total annual precipitation was 842.1–1,717.6 mm, for which erosive precipitation accounted for 78.6% on average. The trends of total annual precipitation, erosive precipitation, and erosivity were evaluated (Figure 3). The precipitation (total/erosive) and erosivity all exhibited an insignificant decreasing trend from 1980 to 2020 ($p > 0.05$). Theil–Sen's slope, which estimates the average rate of change of total and erosive precipitation, was –19.3 and –28.1 mm per decade, respectively (Figure 3(a) and 3(b)). The annual rainfall erosivity had very significant positive correlations with both total and erosive precipitation ($r = 0.89,\ 0.88,\ p < 0.01$), which decreased by –79.0 MJ mm ha^{-1} h^{-1} 10 y^{-1} (Figure 3(c)).

Figure 4 shows the change in the amount and erosivity of each category of erosive precipitation from 1980 to 2020. The heavy precipitation exhibited a decreasing trend of 21.4 mm per decade ($p < 0.05$), and correspondingly, the heavy rainfall erosivity also had a downward trend with a decline of 131.8 MJ mm ha^{-1} h^{-1} 10 y^{-1}.

The M-K test results for the heavy precipitation and erosivity are presented in Figure 5, suggesting that the abrupt change point can be identified around the year 2002. This confirms the significant impact of the reservoir impoundment on local precipitation since 2003. The changes in trends of light, moderate, and very heavy precipitation and erosivity were not statistically significant.

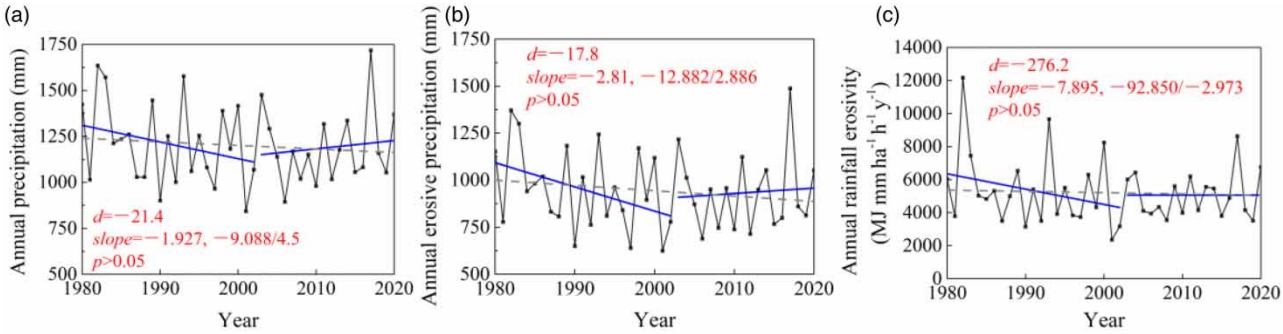

Figure 3 | Interannual variability in annual precipitation, erosive precipitation, and erosivity (*Gray dash lines*: linear trend with Theil–Sen's slope estimated for 1980–2020 period; *blue lines*: linear trend with Theil–Sen's slope estimated for pre- (1980–2002) and post- impoundment (2003–2020) periods; *d*-value: the difference between the averages; *slope*: linear trend estimated via Theil–Sen's slope for the entire period, pre-/post-period.) Please refer to the online version of this paper to see this figure in colour: https://dx.doi.org/10.2166/nh.2022.038.

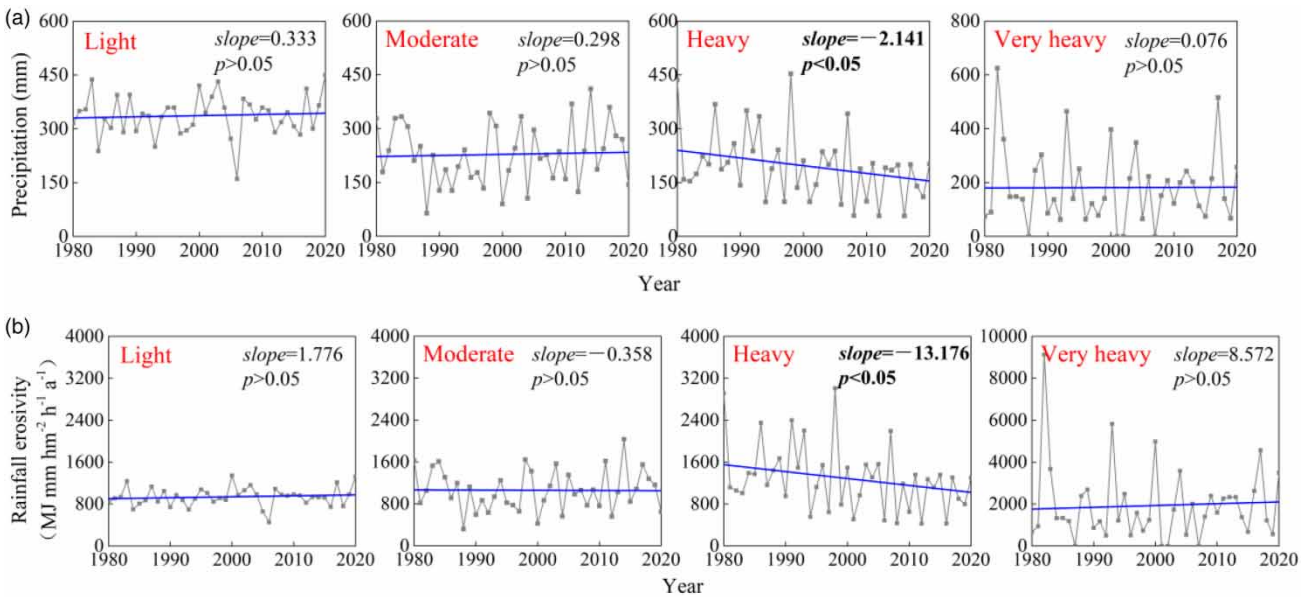

Figure 4 | Time-series trend of light, moderate, heavy, and very heavy precipitation and the corresponding erosivity. *Blue lines*: linear trend with Theil–Sen's slope estimate; *slope*: Theil–Sen's slope; *p*-value: the trend significance from the Mann–Kendall test. (a) Precipitation. (b) Erosivity. Please refer to the online version of this paper to see this figure in colour: https://dx.doi.org/10.2166/nh.2022.038.

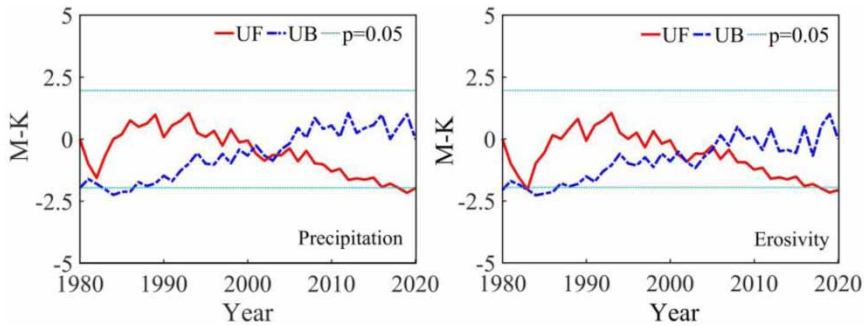

Figure 5 | Mann–Kendall test of the heavy precipitation and corresponding erosivity. The UF represents the statistical series of the standard normal distribution, and the UB represents the reverse statistical series.

Variations between pre- and post-impoundment periods

The mean value of changes in the precipitation amount and erosivity for the erosive precipitations and the four categories, in the pre- and post-impoundment periods, are shown in Figure 6. After the TGR began to store water in 2003, the average erosive precipitation decreased by 17.8 mm while the average rainfall erosivity showed a decrease of 276.2 MJ mm ha^{-1} h^{-1} y^{-1}.

The results indicated that the most significant influence of reservoir impoundment was on the heavy precipitation category. The average annual heavy precipitation amount during the post-impoundment period decreased by 55.2 mm, which shows a reduction of 24.9% compared with that before impoundment ($p < 0.05$). Furthermore, the rainfall erosivity was reduced by 24.3% (350.6 MJ mm ha^{-1} h^{-1} 10 y^{-1}). In addition, the moderate precipitation and erosivity increased by 11.8 and 8.2%, respectively.

Comparing the trend changes between the pre- and post-impoundment periods for the total and erosive precipitation (Figure 3), Theil–Sen's slope indicated that all the trends became weaker after the impoundment since the absolute values of the slopes decreased. The coefficient of variation (*Cv*) indicates the degree of fluctuation of interannual variation. As Table 1 shows, *Cv* of total and erosive precipitation during the post-impoundment period (2003–2020) had a slight decrease within 0.01–0.02, while the *Cv* of rainfall erosivity decreased by 0.16, which indicates the fluctuation degree of annual precipitation and erosivity has been reduced after the reservoir had been impounded. It can also be observed in Figure 3 that especially from 2004 to 2016, the fluctuations of precipitation and rainfall erosivity tended to be stable.

Table 1 presents the *Cv* values of the light, moderate, and heavy precipitation and their corresponding erosivity differing in the range of 0.01–0.05 in the pre- and post-impoundment periods while the same parameters for the very heavy precipitation

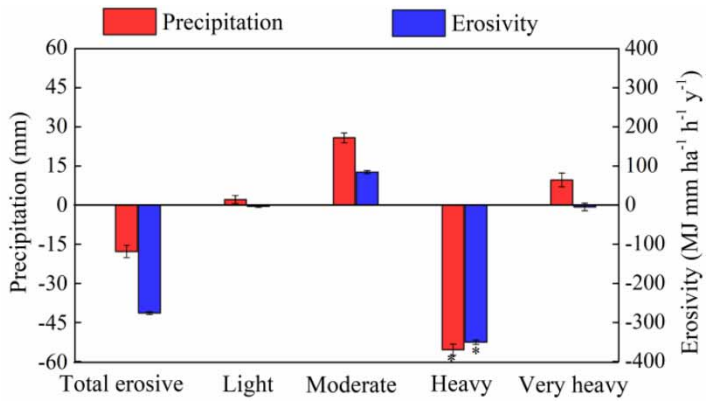

Figure 6 | Mean value of changes in the precipitation amount and erosivity for the four intensities of precipitation between the pre- and post-impoundment periods.

Table 1 | Variable coefficients of rainfall characteristics before and after reservoir storage

Year		1980 ~ 2002	2003 ~ 2020
Precipitation (mm)	Annual	0.19	0.17
	Erosive	0.23	0.22
	Light	0.15	0.20
	Moderate	0.37	0.36
	Heavy	0.47	0.46
	Very heavy	0.90	0.63
	Rx1day	0.40	0.27
	Rx5day	0.46	0.25
Rainfall erosivity (MJ mm ha^{-1} h^{-1} y^{-1})	Annual	0.43	0.27
	Light	0.17	0.22
	Moderate	0.37	0.36
	Heavy	0.49	0.44
	Very heavy	1.13	0.61
	Rx1day	0.79	0.46
	Rx5day	1.00	0.45

category decreased by 0.27 and 0.51, respectively, after the reservoir impoundment. The results indicated that the degree of interannual fluctuation of very heavy precipitation and erosivity is clearly reduced. It can also be seen intuitively from Figure 4(b) that from 2003 to 2020, except for 2017, the annual very heavy rainfall erosivity fluctuated between 0 and 4,560.4 MJ mm ha^{-1} h^{-1} 10 y^{-1} while before 2003 it had fluctuated between 0 and 9,121.4 MJ mm ha^{-1} h^{-1} 10 y^{-1}.

Based on the results above, it is inferred that the reservoir impoundment not only reduced the heavy precipitation but also partially transformed it into moderate precipitation. Although the reservoir storage had little effect on the annual average amount and proportion of the very heavy precipitation and erosivity, the interannual variations had been modified in that the distributions became smoother during the post-impoundment period.

Erosivity contribution of different intensities of precipitation

The probability distribution functions (PDFs) of percentages of light, moderate, heavy, and very heavy precipitation in erosive precipitation and the corresponding erosivity are shown in Figure 7. Throughout the time period of 1980–2020, with the rise of intensity category, the average precipitation proportion decreased from 35.7 to 19.2% while the erosivity proportion increased from 18.0 to 37.0%. Heavy and very heavy precipitation (≥95th percentile) contributed 40.1% of the erosive precipitation with very little frequency (6.2 d), and 61.7% of the rainfall erosivity. Therefore, in the TGR area, heavy and very heavy precipitation should be paid special attention to because of their significant erosivity.

The distribution of moderate precipitation and erosivity percentage both showed a noticeable shift toward the right of the peak distribution during the post-impoundment period, indicating that the moderate precipitation percentage increased in the 2003–2020 period (Figure 7(a)). During the post-impoundment period, the proportion of moderate precipitation was mainly distributed between 22 and 26%, and the average proportion has increased by 2.9% compared with that before the impoundment. For heavy precipitation, the PDF had a significant rise and shifted toward the left of the peak location in the second period (Figure 7(a)), implying that the heavy precipitation percentage decreased ($p < 0.05$). After the reservoir impoundment, the proportion of heavy precipitation was concentrated around 18–20%, and the annual average proportion was 5.5% lower than that before the impoundment. Meanwhile, the rise of the PDF curve of moderate and heavy categories indicated that the proportions were more concentrically distributed and had a decrease in interannual variation. The proportions of light and very heavy precipitation did not change much before and after the impoundment, with an average annual proportion of 36.8 and 18.2%, respectively.

The erosivity proportion had the same change as that of the precipitation proportion (Figure 7(b)). The moderate rainfall erosivity proportion showed a right shift with respect to the peak distribution while the PDF curve of the heavy rainfall erosivity proportion presented a left shift in the post-impoundment period ($p < 0.05$). The average annual proportion of

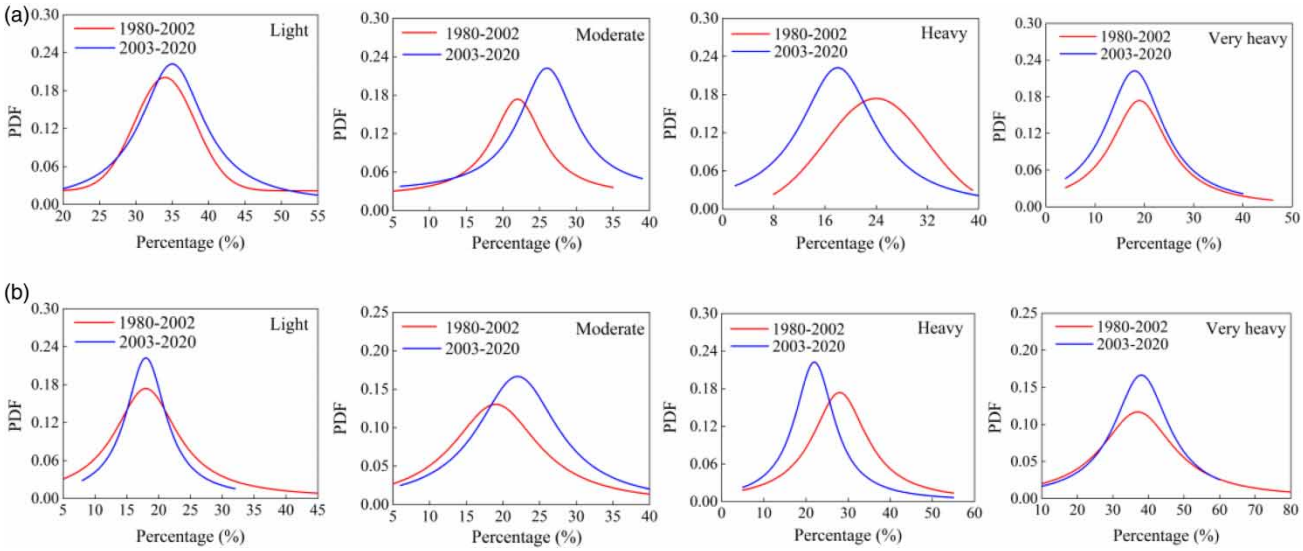

Figure 7 | Probability distribution functions of percentages of light, moderate, heavy, and very heavy precipitation and corresponding erosivity. (a) Precipitation. (b) Erosivity.

moderate and heavy rainfall erosivity was 2.7% higher and 5.5% lower than that before the impoundment, respectively. The results indicated that since the reservoir impoundment, there has been a tendency to transform from heavy precipitation and erosivity to moderate category, in local erosive precipitation.

Seasonal variation in the amount and erosivity of different intensities of precipitation

Monthly distribution

The monthly distributions of precipitation, erosive precipitation, and rainfall erosivity are presented in Figure 8. During the pre-impoundment period, the total monthly and erosive precipitation presented a unimodal distribution with a peak in July. The two precipitation indices were mainly distributed from May to September, with a proportion sum of 71.8 and 79.5% of total annual and erosive precipitation, respectively (Figure 8(a)). The monthly erosivity also showed changes similar to the precipitation, which was mainly distributed from May to September, with a proportion of 88.5% of the total annual erosivity (Figure 8(c)). However, after the reservoir had begun to store water (2003), the monthly distribution of the precipitation and erosivity all presented a bimodal distribution with two peaks in July and September (Figure 7(b) and 7(c)). Precipitation and erosive precipitation were still mainly concentrated from May to September, but the distribution tended to be uniform between these months with proportions of 68.8 and 75.2% (Figure 8(b)). Especially for rainfall erosivity, it was highly concentrated in July before the reservoir impoundment (Figure 3(c)) but tended to be uniformly distributed from May to September during the post-impoundment period, with a proportion of 85.7%.

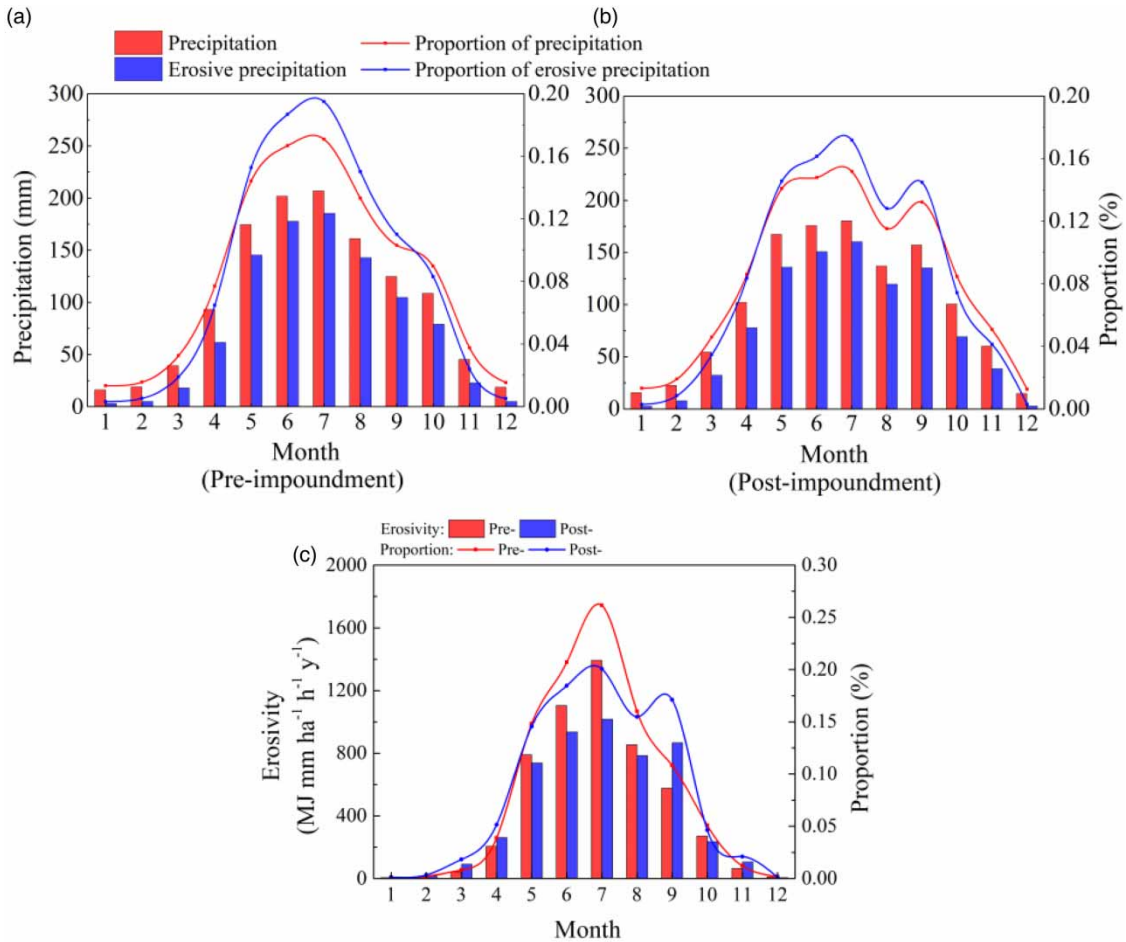

Figure 8 | Monthly distribution of precipitation, erosive precipitation, and erosivity during pre- (1980–2002) and post-impoundment (2003–2020) periods. Numbers from 1 to 12 mean the month from January to December.

Seasonal distribution

In order to further understand the impact of the TGR impoundment on the adjustment of the local annual precipitation distribution, the rainfall characteristics were analyzed by seasons, including March to May (spring), June to August (summer), September to November (autumn), December, January, and February (winter). The interannual variability of precipitation and erosivity in the TGR area was mainly contributed by summer rainfall and erosivity. On average, the summer precipitation accounted for 44.7% of the annual rainfall (Figure 9), and the average rainfall erosivity was 3,082.6 MJ mm ha^{-1} h^{-1} y^{-1}, accounting for 59.2% of the annual erosivity. The erosivity proportions in spring and autumn were similar, being 20.4 and 20.0%, respectively. The winter precipitation was the least among the seasons, accounting for 0.5%.

Among precipitations of different categories (Figure 9), the moderate, heavy, and very heavy rainfall events all occurred mainly in summer. The precipitation distributions in summer were all more than half of the precipitation (50.6, 56.1, and 67.5%) while there was no distribution in winter. Furthermore, the erosivity distribution was even more prominent in summer, accounting for 53.4, 57.6, and 71.8% of their total erosivity.

Seasonal changes between the pre- and post-impoundment periods

After the reservoir was impounded, the proportion of total precipitation and erosivity in spring and winter almost remained the same while the changes were more obvious in summer and autumn (Figure 10). The precipitation distribution was reduced by 5.9% in summer, and the corresponding erosivity distribution was decreased by 8.9% while in the autumn, precipitation and erosivity distributions increased by 4.2 and 6.7%, respectively. Therefore, it can be concluded that the seasonal distribution of annual rainfall changed after the reservoir was impounded and summer rainfall and erosivity shifted to autumn.

For the four categories of precipitation, it can be observed that the light precipitation and its erosivity in spring were increased by 5.5 and 5.0% after the reservoir was impounded ($p < 0.05$) while the distributions in summer and autumn were slightly reduced (by 1.8–3.4%). Although the distribution of the erosivity of the medium, heavy, and very heavy

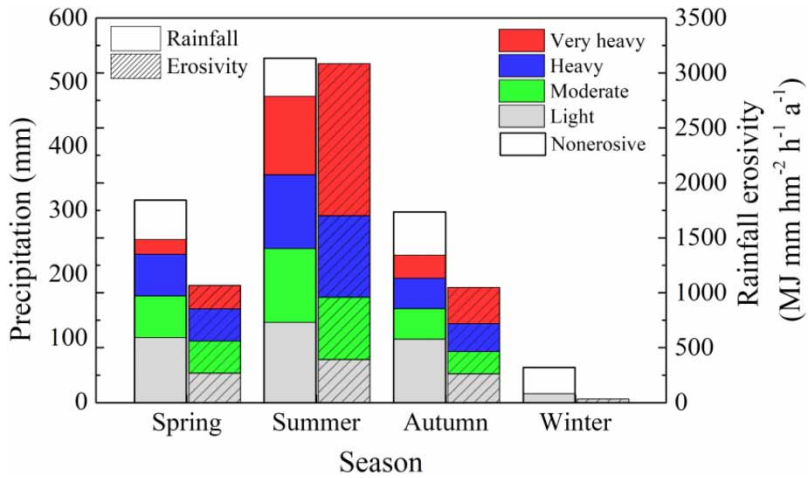

Figure 9 | Mean precipitation and rainfall erosivity in each season.

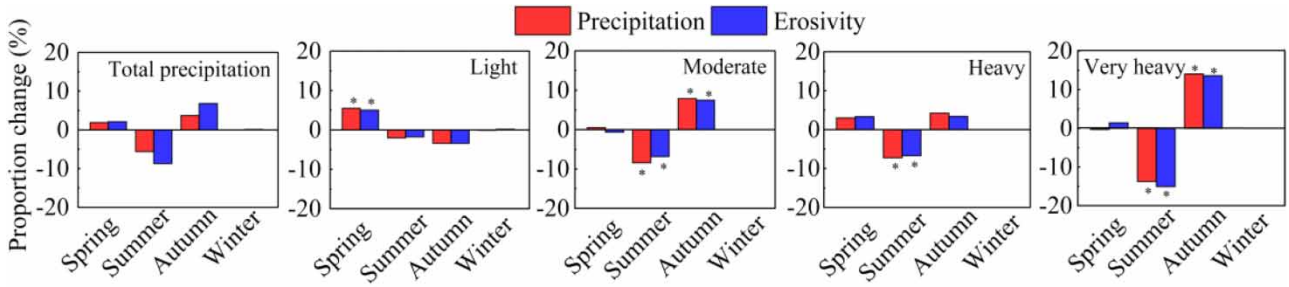

Figure 10 | Changes of the distributed proportion of total precipitation and four intensities of precipitations in each season in the two periods of pre- (1980–2002) and post-impoundment (2003–2020).

precipitation in summer decreased to varying degrees, they all increased in autumn. Among the categories, the erosivity distribution of the very heavy rainfall changed the most. It decreased by 15.0% in summer and increased by 13.6% in autumn, as the result of a decrease of 13.8% in the precipitation distribution in summer and an increase of 14.0% in autumn. The distribution of moderate precipitation shifted mainly from summer to autumn with a decrease of 8.4% in summer and an increase of 7.2% in autumn, leading to a 7.5% increase in the distribution of the erosivity in autumn. The distributions of the heavy precipitation and erosivity were mainly transferred evenly from summer to spring and autumn and were reduced by 7.2 and 6.7%, respectively, in summer.

The results showed that the transfer of summer precipitation and erosivity to autumn after the reservoir impoundment was mainly reflected in precipitation except for the low-intensity case, with the very heavy precipitation being affected the most. Therefore, the impoundment of the reservoir changed the previous highly centralized distribution of the precipitation of higher intensity in summer and made it more evenly distributed between the seasons. Meanwhile, the risk of soil erosion in summer was reduced, but the entire high-risk period was extended to span the summer and autumn.

Change in Rx1day, Rx5day, and the corresponding erosivity

As Figure 11 shows, from 1980 to 2020, the Rx1day in the central area of the TGR, Wanzhou District, was in the range of 55.4–199.3 mm while the Rx5day was in the range of 71.9–399.0 mm, accounting for 7.8 and 12.7% of the annual rainfall, respectively. On the other hand, regarding rainfall erosivity, these parameters accounted for 20.3 and 25.6% of the annual erosivity, respectively. The Theil–Sen's slope (Figure 11) indicated that during the entire period, the changes in trends of Rx1day and Rx5day and their corresponding erosivity were not statistically significant. However, it is worth noting that after 2002, the fluctuations of Rx1day and Rx5day and the relative erosivity were significantly reduced (Figure 10). Table 1 shows that the *Cv* of Rx1day and Rx5day decreased by 0.14 and 0.24 for the post-impoundment period while for the relative erosivity, it decreased by 0.33 and 0.54. The decrease in *Cv* confirmed that the interannual fluctuations of the extreme rainfall and its erosivity were weakened after the reservoir was impounded whereas the smoothing of the Rx5day indicator is more significant.

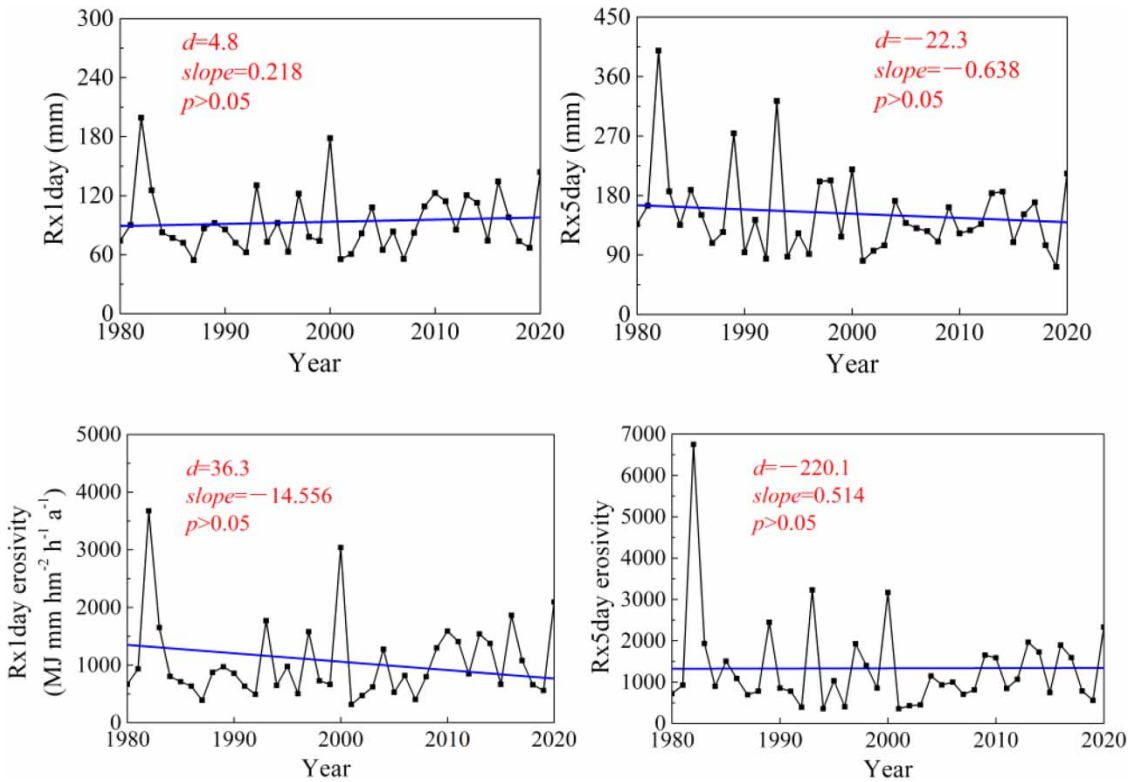

Figure 11 | Time-series trend of Rx1day, Rx5day, and the corresponding erosivity (*Blue lines*: Theil–Sen's slope for the linear trend estimated for the 1980–2020 period; *d-value*: the difference between the mean values of pre- (1980–2002) and post-impoundment (2003–2020) periods). Please refer to the online version of this paper to see this figure in colour: https://dx.doi.org/10.2166/nh.2022.038.

During the pre-impoundment period from 1980 to 2002, there are four obvious peaks in Rx1day erosivity: 3,675.1 (in 1982), 969.3 (in 1989), 1,769.2 (in 1993), 1,577.2 (in 1997), and 3,038.2 (in 2000) MJ mm ha^{-1} h^{-1} 10 y^{-1}, accounting for 30.2, 18, 42.4, and 36.9% of the total erosivity in the corresponding years, respectively. Rx5day erosivity had five obvious peaks: 6,749.6 (in 1982), 2,445.9 (in 1989), 3,227.3 (in 1993), 1,927.6 (in 1997), and 3,168.8 (in 2000). The corresponding erosivity accounted for 55.5, 37.4, 33.4, 51.8, and 38.5% of the total erosivity in the corresponding years, respectively. It can be observed that in the case of extreme rainfall, the erosivity of one rainfall or several consecutive days of rainfall in the TGR area can account for nearly half or even more than half of the annual erosivity. After the reservoir was impounded (2003–2020), the extreme rainfall and its erosivity changed relatively smoothly. The maximum values of Rx1day and Rx5day (in 2020) are respectively 8.7 and 24.7% lower than the average peak values before impoundment. The relative peak values of Rx1day and Rx5day erosivity are 16.7.0 and 33.5% of the average peak values before impoundment. Therefore, the water storage of the reservoir may have the effect of removing the peak and evenly distributing the extreme rainfall. During the post-impoundment period, the extreme rainfall peak values were reduced by 12.7% on average, whereas the erosivity peak values were reduced by 25.1% on average.

DISCUSSION

Annual changes between pre- and post-impoundment periods

Our results indicated a significant influence of the reservoir impoundment on the local precipitation in the TGR area. Distinctive changes existed in the heavy precipitation category (95th–99th percentile). It had a significant decline trend and most of the reduction caused a shift into the moderate category (85th–95th percentile). This result coincided with the findings of Wu *et al.* (2016) for all of China, that higher precipitation intensities had higher rates of change. The abrupt point by the M-K test was around the year 2002 (Figure 5), which is evidence of the significant effect of the reservoir impoundment (in 2003) on the local precipitation. Both the total precipitation and erosivity presented decreasing trends, which is in line with the conclusion of Wu *et al.* (2006) who stated that the precipitation increased in the region between Daba and Qinling Mountains, whereas the precipitation in the vicinity of the Yangtze River was reduced after the impoundment in June 2003. However, in the present findings, the mean precipitation did not differ greatly ($p > 0.05$) after the filling of the TGD, which confirmed the simulation by Miller *et al.* (2005), suggesting that there was no significant change in annual precipitation.

The changes were mainly due to the land use and land cover alterations caused by the reservoir impoundment, which altered the probability of precipitation being harvested from local evaporation in precipitation recycling (Hossain *et al.* 2009). After reservoir impoundment, the water surface increased by 397.1 km^2 (He *et al.* 2020), hence, it is physically plausible that the increased evaporation from the open-water surface of a reservoir will feed precipitation through a feedback mechanism (Eltahir 1989). On the other hand, the evaporating surface decreased the local surface temperature leading to sinking air (Miller *et al.* 2005), which limited the supply to precipitation.

Moreover, in the TGR, the land use area covered by vegetation aggregately decreased by 1,196.6 km^2 over the period of 1990–2015, including dry croplands, paddy fields, grasslands, and forests while the built-up area increased by 799.5 km^2 (He *et al.* 2020). The alteration in the spatial pattern of transpiration and evaporation due to the land cover change resulted in a reduction in water flux to the atmosphere, leading to less precipitation from thunderstorms and a spatial displacement in the rainfall pattern (Pielke & Walko 1999). Therefore, although large-scale surface evaporation can trigger changes in precipitation recycling, the reduction of transpiration and evaporation may dominate the feedback mechanism. As a result, the annual precipitation demonstrated a declining trend. Meanwhile, the reduction of the water flux into the atmosphere after the reservoir impoundment also led to a reduction in the rainfall of a single rainstorm. Therefore, the heavy rainfall peaks were significantly eliminated and mostly shifted into moderate rainfalls. However, the erosivity of heavy precipitation has not been transferred into the moderate category to the same extent, the former decreased by 24.3%, and the latter increased by only 8.2% after the water was impounded. Hence, the reservoir impoundment obviously mitigated the erosion threat of the heavy rainfalls in the TGR and also reduced the risk of annual erosion.

Seasonal change

The monsoon season of the TGR occurs from May to September, when the temperature is high and rainfall is necessary to compensate for intense evaporation (Fang *et al.* 2010). Therefore, most precipitation, as well as the heaviest rainfall events, occur in summer. However, due to the predominant effect of the reduced area of plant transpiration after the impoundment, especially in summer when the transpiration is the strongest, summer precipitation decreased. This is similar to the results

presented by the study of Zhang *et al.* (2015) in Guangdong Province, China, indicating that not only precipitation in summer was decreasing overall, but also that a wetting tendency of the winter, spring, and autumn existed due to the water reservoirs. Among the four intensity categories, the very heavy precipitation contributed the most (decreased by 15.0% in proportion in summer) to the decline of summer precipitation. The weaker rainstorm led to a weaker fluctuation of the summer precipitation, which was also due to the reduction of the water flux into the atmosphere after the reservoir impoundment.

The replenishment of atmosphere water flux by reservoir surface evaporation in autumn was obviously greater than that before impoundment. Therefore, autumn precipitation, especially for very heavy precipitation cases, increased. The unimodal distribution of monthly rainfall before the impoundment had also changed to a bimodal distribution, with the second peak in September (Figure 8). As a result of the seasonal precipitation variation after the water was impounded, rainfall erosivity was no longer highly concentrated in summer, causing a very high level of erosion risk in July. Instead, the erosivity was evenly distributed in the summer and autumn (May–September) and the erosion risk period was less threatening than before the impoundment. Therefore, the change from one erosivity peak in July before impoundment to two peaks in July and September indicates that the risk of soil erosion is reduced, but now there are two risk periods to focus on each year.

Rainfall extremes and the relative erosivity contribution

After the reservoir impoundment, it is physically plausible that the intense evaporation from the vast water surface will alter extreme precipitation patterns through a feedback mechanism (Hossain *et al.* 2009). In our results, after the water was impounded, the most notable change in extreme rainfall was the flattening of fluctuations. The peak values of the Rx1day and Rx5day were reduced by 8.7 and 24.7%, respectively, verifying the reduction of the water flux into the atmosphere after the reservoir impoundment.

Besides, in the present study, very heavy precipitation is also counted as one extreme indicator since it is classified as the top 1% of the rainfall events, which is the R99p among the commonly used indices (Wang *et al.* 2017). Likewise, the fluctuation degree of the very heavy precipitation was reduced obviously after the impoundment (Figure 4(a)), except for an extreme value in 2017. In the autumn of 2017, the subtropical high has been maintained along the Yangtze River in Chongqing and the middle and lower reaches of the Yangtze River for a long time. The middle and high latitudes maintained a double resistance type, slowing the western low trough to move eastward, which resulted in frequent abnormally heavy precipitation in Chongqing from September to October (Tang *et al.* 2019). Therefore, if excluding the impact of extreme climate in 2017, the fluctuating degree reduced by 42.2%. That is, the flattening and peak-cutting effects of reservoir impoundment on extreme precipitation were more outstanding.

However, many studies demonstrated that an increasing trend of extreme precipitation has emerged under global warming (Trenberth *et al.* 2015; Donat *et al.* 2017). The present study indicates that, under the influence of the reservoir impoundment, the change of trend of the extreme rainfall was not specific. This is consistent with the finding of Song *et al.* (2020) indicating that the TGR impoundment has not significantly affected the storm patterns.

The precipitation from the very heavy category (99th percentile) is characterized by relatively short duration and high intensity that occurred approximately twice a year and contributed to more than one-third of the annual erosivity in the TGR. The same situation existed in Rx1day and Rx5day. Previous studies noted that soil loss was highly sensitive to precipitation types with short durations and very high intensities, which would result in severe land degradation (Martin *et al.* 2016; Strohmeier *et al.* 2016). However, after the reservoir impoundment, the previous extreme rainfalls were reduced and smoothed in the TGR, suggesting that the reservoir impoundment eliminated the threat from a few extreme precipitation events. Although the narrow spatial constraints of the investigation may limit the generality of the results and conclusions, this study provides evidence of a significant effect of TGR impoundment on local precipitation.

CONCLUSION

The influence of the reservoir impoundment of the TGR since 2003 on local precipitation and rainfall erosivity was investigated in the present study. The impoundment has had a significant impact on local precipitation, which is mainly reflected in the heavy precipitation (95th–99th percentile) and the relative erosivity. Both of these parameters displayed a significant decline trend from 1980 to 2020 ($p < 0.05$). The abrupt point indicated by the M-K test was around the year 2002, which is evidence of the significant effect of the reservoir impoundment on the local precipitation. Reservoir impoundment redistributed the intensity levels of erosive precipitation in which the precipitation and erosivity both shifted from the heavy to the moderate category. After the impoundment, the annual heavy precipitation was reduced by 24.9% and the relative

erosivity decreased by 24.3% averagely ($p < 0.05$). The moderate precipitation and erosivity both increased by 11.8 and 8.2%, respectively.

The impoundment of the TGR also caused a trend of precipitation shift from summer to autumn. As a result, the unimodal distribution of monthly precipitation and erosivity had been altered to a bimodal distribution, resulting in a longer but lower-risky erosion period of high concern. The most significant effect of reservoir impoundment on extreme rainfall lies in the peak cutting and flattening effect. The interannual fluctuations of Rx1day and Rx5day have been significantly reduced after reservoir impoundment, with a peak clipping of 12.7%, and correspondingly 25.1% on the rainfall erosivity on average.

ACKNOWLEDGEMENTS

This work was supported by the Natural Science Foundation of China (U2040207) and the Sichuan Science and Technology Program (2020YFQ0002/2022YFS0493).

DATA AVAILABILITY STATEMENT

Data cannot be made publicly available; readers should contact the corresponding author for details.

CONFLICT OF INTEREST

The authors declare there is no conflict.

REFERENCES

Degu, A., Hossain, F., Niyogi, D., Pielke, R., Shepherd, J., Voisin, N. & Chronis, T. 2011 The influence of large dams on surrounding climate and precipitation patterns. *Geophysical Research Letters* **38**, L04405. https://doi.org/10.1029/2010GL046482.

Donat, M., Lowry, A., Alexander, L., O'Gorman, P. & Maher, N. 2017 More extreme precipitation in the world's dry and wet regions. *Nature Climate Change* **6**, 508–513. https://doi.org/10.1038/NCLIMATE3160.

Eltahir, E. 1989 A feedback mechanism in annual rainfall, Central Sudan. *Journal of Hydrology* **110**, 323–334. https://doi.org/10.1016/0022-1694(89)90195-9.

Fang, Z., Hang, D. & Zhao, X. 2010 Rainfall regime in Three Gorges area in China and the control factors. *International Journal of Climatology* **30**, 1396–1406. https://doi.org/0.1002/joc.1978.

Gangoiti, G., Gómez-Domenech, I., Cámara, E., Alonso, L., Navazo, M., Jza, J., García, J., Ilardia, J. & Millán, M. 2011 Origin of the water vapor responsible for the European extreme rainfalls of August 2002: 2. A new methodology to evaluate evaporative moisture sources, applied to the August 11–13 central European rainfall episode. *Journal of Geophysical Research: Atmospheres* **116**, D21103. https://doi.org/10.1029/2010JD015538.

Gu, Z., Duan, X., Liu, B., Hu, J. & He, J. 2016 The spatial distribution and temporal variation of rainfall erosivity in the Yunnan Plateau, Southwest China: 1960–2012. *CATENA* **145**, 291–300. http://dx.doi.org/10.1016/j.catena.2016.06.028.

He, X., Wang, M., Tang, Q., Bao, Y., Li, J. & Dil, K. 2020 Decadal loss of paddy fields driven by cumulative human activities in the Three Gorges Reservoir area, China. *Land Degradation & Development* **31**, 1–13. https://doi.org/10.1002/ldr.3574.

Hossain, F., Jeyachandran, I. & Sr. Pielke, R. 2009 Have large dams altered extreme precipitation patterns? *Eos Transactions American Geophysical Union* **90**, 453–454. https://doi.org/10.1029/2009eo480001.

Hossain, F., Jeyachandran, I. & Pielke, R. 2010 Dam safety effects due to human alteration of extreme precipitation. *Water Resources Research* **46**, W03301. https://doi.org/10.1029/2009WR007704.

Hsu, P., Lee, J. & Ha, K. 2016 Influence of boreal summer intraseasonal oscillation on rainfall extremes in southern China. *International Journal of Climatology* **36**, 1403–1412. https://doi.org/10.1002/joc.4433.

Keller, P., Marcé, R., Obrador, B. & Koschorreck, M. 2021 Global carbon budget of reservoirs is overturned by the quantification of drawdown areas. *Nature Geoscience* **14**, 402–408. https://doi.org/10.1038/s41561-021-00734-z.

Kendall, M. G. 1975 *Rank Correlation Methods*, 4th edn. Charles Griffin, London.

Liu, H., Zhang, G., Zhang, P. & Zhu, S. 2020 Spatial distribution and temporal trends of rainfall erosivity in Three Gorges Reservoir Area of China. *Mathematical Problems in Engineering* **2020**, 15. https://doi.org/10.1155/2020/5302679.

Lv, M., Yi, J., Chen, X., Chen, J., Wu, S. & Liu, J. 2018 Spatiotemporal variations of extreme precipitation under a changing climate in the Three Gorges Reservoir Area (TGRA). *Atmosphere* **9**, 24. https://doi.org/10.3390/atmos9010024.

Mann, H. 1945 Nonparametric tests against trend. *Econometrica* **13**, 245–259. https://doi.org/10.2307/1907187.

Martin, H., Alena, P. & Jan, K. 2016 Trends in characteristics of sub-daily heavy precipitation and rainfall erosivity in the Czech Republic. *International Journal of Climatology* **36**, 1833–1845. https://doi.org/10.1002/joc.4463.

Miller, N., Jin, J. & Tsang, C. 2005 Local climate sensitivity of the Three Gorges Dam. *Geophysical Research Letters*. https://doi.org/10.1029/2005GL022821

Pendergrass, A., Knutti, R., Lehner, F., Deser, C. & Sanderson, B. 2017 Precipitation variability increases in a warmer climate. *Scientific Reports* **7**, 17966. https://doi.org/10.1038/s41598-017-17966-y.

Pielke, R. & Walko, R. 1999 The influence of anthropogenic landscape changes on weather in south Florida. *American Meteorological Society* **127**, 1663–1673. http://dx.doi.org/10.1175/1520-0493(1999)127 < 1663:tioalc > 2.0.co;2.

Pizarro, R., Garcia-Chevesich, P., Valdes, R., Dominguez, F., Hossain, F., Ffolliott, P., Olivares, C., Morales, C., Balocchi, F. & Bro, P. 2013 Inland water bodies in Chile can locally increase rainfall intensity. *Journal of Hydrology* **481**, 56–63. http://dx.doi.org/10.1016/j.jhydrol.2012.12.012.

Sen, P. 1968 Estimates of the regression coefficient based on Kendall's tau. *Publications of the American Statistical Association* **63**, 1379–1389. http://dx.doi.org/10.1080/01621459.1968.10480934.

Shi, D., Jiang, G., Peng, X., Jin, H. & Jiang, N. 2021 Estimates of the relationship between the periodicity of soil and water loss and erosion-sensitive periods based on temporal distributions of rainfall erosivity in the Three Gorges Reservoir Region, China. *Catena* **202**, 105268. http://dx.doi.org/10.1016/j.catena.2021.105268.

Shin, J., Kimb, T., Heob, J. & Lee, J. 2019 Spatial and temporal variations in rainfall erosivity and erosivity density in South Korea. *Catena* **176**, 125–144. https://doi.org/10.1016/j.catena.2019.01.005.

Song, J., Ma, L., Her, Y. & Li, Y. 2020 Immediate influences of a large dam construction on local storm event patterns and weather variables: a case study of the Three Gorges Project. *Weather* **99**, 99–103. https://doi.org/10.1002/wea.3410.

Strohmeier, S., Laaha, G., Holzmann, H. & Klik, A. 2016 Magnitude and occurrence probability of soil loss: a risk analytical approach for the plot scale for two sites in lower Austria. *Land Degradation & Development* **27**, 43–51. https://doi.org/10.1002/ldr.2354.

Tang, H., Wu, Y. & Dong, X. 2019 Causes analyses of precipitation anomaly in Chingqing in autumn 2017. *Meteorological Monthly* **45**, 799–810. CNKI:SUN:QXXX.0.2019-06-006 (in Chinese with English abstract).

Theil, H. 1992 *A Rank-Invariant Method of Linear and Polynomial Regression Analysis*. Springer Netherlands, Netherlands.

Trenberth, K., Fasullo, J. & Shepherd, T. 2015 Attribution of climate extreme events. *Nature Climate Change* **5**, 725–730. https://doi.org/10.1038/nclimate2657.

Wang, X., Hou, X. & Wang, Y. 2017 Spatiotemporal variations and regional differences of extreme precipitation events in the coastal area of China from 1961 to 2014. *Atmospheric Research* **197**, 94–104. https://doi.org/10.1016/j.atmosres.2017.06.022.

Woldemichael, A., Hossain, F. & Pielke, R. 2014 Impacts of postdam land use/land cover changes on modification of extreme precipitation in Contrasting Hydroclimate and Terrain Features. *Journal of Hydrometeorology* **15**, 777–800. https://doi.org/10.1175/JHM-D-13-085.1.

Wu, L., Zhang, Q. & Jiang, Z. 2006 Three Gorges Dam affects regional precipitation. *Geophysical Research Letters* **33**, L13806. https://doi.org/10.1029/2006GL026780.

Wu, Y., Wu, S., Wen, J., Ming, X. & Tan, J. 2016 Changing characteristics of precipitation in China during 1960–2012. *International Journal of Climatology* **36**, 1387–1402. https://doi.org/10.1002/joc.4432.

Xiao, C., Yu, R. & Fu, Y. 2010 Precipitation characteristics in the Three Gorges Dam vicinity. *International Journal of Climatology* **30**, 2021–2024. https://doi.org/10.1002/joc.1963.

Xiao, Q., Xiao, Y. & Tan, H. 2020 Changes to soil conservation in the Three Gorges Reservoir Area between 1982 and 2015. *Environmental Monitoring and Assessment* **192**, 44. https://doi.org/10.1007/s10661-019-7983-1.

Xie, Y., Yin, S. Q., Liu, B. Y., Nearing, M. A. & Zhao, Y. 2016 Models for estimating daily rainfall erosivity in China. *Journal of Hydrology* **535**, 547–558. http://dx.doi.org/10.1016/j.jhydrol.2016.02.020.

Xu, X., Tan, Y. & Yang, G. 2013 Environmental impact assessments of the Three Gorges Project in China: issues and interventions. *Earth-Science Reviews* **124**, 115–125. http://dx.doi.org/10.1016/j.earscirev.2013.05.007.

Xu, X., Lyu, D., Lei, X., Huang, T., Li, Y., Yi, H., Guo, J., He, L., He, J., Yang, X., Guo, M., Liu, B. & Zhang, X. 2021 Variability of extreme precipitation and rainfall erosivity and their attenuated effects on sediment delivery from 1957 to 2018 on the Chinese Loess Plateau. *Journal of Soils and Sediments* **21**, 3933–3947. https://doi.org/10.1007/s11368-021-03054-2.

Yao, J., Chen, Y., Chen, J., Zhao, Y. & Mao, W. 2020 Intensification of extreme precipitation in arid Central Asia. *Journal of Hydrology* **598**, 125760. https://doi.org/10.1016/j.jhydrol.2020.125760.

Yigzaw, W., Hossain, F. & Kalyanapu, A. 2012 Impact of artificial reservoir size and land use/land cover patterns on probable maximum precipitation and flood: case of Folsom Dam on the American River. *Journal of Hydrologic Engineering* **18**, 1180–1190. https://doi.org/10.1061/(ASCE)HE.1943-5584.0000722.

Yin, S., Xue, X., Yue, T., Xie, Y. & Gao, G. 2019 Spatiotemporal distribution and return period of rainfall erosivity in China. *Transactions of the Chinese Society of Agricultural Engineering* **35**, 9. https://doi.org/10.11975/j.issn.1002-6819.2019.09.013.

Zhang, Q., Xiao, M., Singh, V., Xu, C. & Li, J. 2015 Variations of annual and seasonal runoff in Guangdong Province, south China: spatiotemporal patterns and possible causes. *Meteorology and Atmospheric Physics* **127**, 273–288. https://doi.org/10.1007/s00703-014-0360-2.

Zhang, T., Wilson, G., Hao, Y. & Han, X. 2021 Erosion hazard evaluation for soil conservation planning that sustains life expectancy of A horizon: the black soil region of China. *Land Degradation and Development* **32**, 2629–2641. https://doi.org/10.1002/ldr.3931.

Zhao, F. & Shepherd, M. 2012 Precipitation changes near Three Gorges Dam, China. Part I: a spatiotemporal validation analysis. *Journal of Hydrometeorology* **13**, 735–745. https://doi.org/10.1175/JHM-D-11-061.1.

First received 28 March 2022; accepted in revised form 30 September 2022. Available online 20 October 2022